PERGAMON

International Journal of Solids and Structures 37 (2000) 5037–5059

INTERNATIONAL JOURNAL OF SOLIDS and STRUCTURES

www.elsevier.com/locate/ijsolstr

Forming limit diagrams for anisotropic metal sheets with different yield criteria

Mitsutoshi Kuroda*, [1], Viggo Tvergaard

Department of Solid Mechanics, Technical University of Denmark, Building 404, DK-2800 Lyngby, Denmark

Received 3 August 1998; in revised form 16 July 1999

Abstract

For thin metal sheets subject to stretching under various in-plane tensile stress histories, localized necking is analyzed by using the M–K-model approach, and forming limit diagrams are drawn based on the critical strains for localization. The analyses account for plastic anisotropy, and predictions are shown based on four different anisotropic plasticity models, which have all been fitted to agree with the same set of experimental data. Situations where the tensile axis is along one of the orthotropic axes of the anisotropy are studied, as well as situations where the tensile axis is inclined to the orthotropic axes. Furthermore, the effect of allowing for nonzero shear strains outside the necking band is considered. In all analyses the rotation of the orthotropic axes is accounted for, and a few studies are used to evaluate the effect of assuming the development of a plastic spin.

Keywords: Constitutive equations; Orthotropy; Instability; Large deformation; Plasticity

1. Introduction

For thin metal sheets subject to in-plane stretching the occurrence of a tensile instability, leading to localized necking in the sheet, is one of the most frequently observed failure mechanisms. In industrial sheet metal forming operations such localized necking is known to be an important limitation on sheet metal formability (Keeler, 1968). In practice, so called forming limit diagrams for a given sheet metal are used to plot the critical strain for localization, corresponding to a range of different stress or strain

* Corresponding author. Present address: Department of Mechanical Systems Engineering, Yamagata University, 4-3-16 Jonan, Yonezawa 992-8510, Japan. Fax: +81-238-26-3205.

E-mail address: kuroda@dip.yz.yamagata-u.ac.jp (M. Kuroda).

[1] On leave from Ashikaga Institute of Technology, Ashikaga, Japan.

0020-7683/00/$ - see front matter
PII: S0020-7683(99)00200-0

histories. There has been much interest in the development of theoretical methods for the prediction of forming limit diagrams.

For an initially uniform sheet described by classical isotropic hardening rigid-plastic theory with a smooth yield surface and normality, Hill (1952) found bifurcation into a localized necking mode, provided that the principal strain increments in the plane of the sheet are of opposite sign. However, no such bifurcations were predicted in the important range, where both principal strain increments are positive. For this range, Marciniak and Kuczynski (1967) have shown by a simple plane stress analysis, often called the M–K-model, that localized necking is predicted if an initial thickness inhomogeneity is assumed in the sheet. This is significant, as inhomogeneities of either thickness or material properties are unavoidable in practice. As an alternative approach, Støren and Rice (1975) assume that a vertex forms on the yield surface and show that for a uniform sheet this leads to bifurcation predictions at realistic strain levels, in the whole range of strain ratios. A noteworthy general feature of these plane-stress analyses for sheet necking is the analogy with the standard formulation used to analyze shear band instabilities in three-dimensional (3D) solids (e.g. see Ref. Tvergaard, 1989). For the uniform 3D problem, the first critical bifurcation into a shear band coincides with loss of ellipticity of the governing differential equations, while in the 2D sheet-necking problem bifurcation corresponds to loss of ellipticity of the plane stress equations.

Forming limit predictions are very sensitive to the constitutive model assumed, as was already shown by Støren and Rice (1975). Subsequently, Tvergaard (1978, 1980) has used a kinematic hardening model to show that the critical strain is very sensitive to the local curvature of the yield surface at the point of loading, if the sheet contains an initial imperfection. Also early studies of the effect of anisotropic plasticity in metal sheets (Parmar and Mellor, 1978; Bassani et al., 1979) have demonstrated a strong sensitivity to small changes of parameters determining the yield surface shape. More recently, Barlat (1987), Barlat and Richmond (1987) and Barlat and Lian (1989) have developed anisotropic yield surfaces representing various crystallographic textures, and such yield surfaces have been used in sheet necking analyses (e.g. Lian et al., 1989a). Also, Lian et al. (1989b), Xu and Weinmann (1998) have used, respectively, the anisotropic yield criteria of Hill (1979, 1993) only in the range where both principal strains are positive. An alternative approach to the study of plastic anisotropy effects on predictions of flow localization relies on the direct use of an elastic-viscoplastic Taylor-type polycrystal model to represent initial textures as well as texture development during deformation (Asaro and Needleman, 1985; Tvergaard and Needleman, 1993). Recently, this approach has been used by Wu et al. (1997, 1998) in a number of detailed sheet necking analyses for rolled aluminum alloy sheets.

In analyzing sheet metal formability it is important to realize that the critical strain for localization is highly path dependent. Most analyses based on the M–K-model, including all those mentioned above, have assumed a fixed ratio of the in-plane principal logarithmic strains during the deformation leading to each point on the forming limit curve. But M–K- model analyses using nonproportional strain paths prior to localization show that the critical strain at localization can be much increased or much reduced by choosing different nonproportional strain paths in the pre-localization deformation (e.g. see Ref. Needleman and Tvergaard, 1984). In real sheet metal forming operations complex geometries or drawing sequences can result in significant deviations from proportional straining, which affect the onset of localization.

The onset of localized necking in anisotropic metal sheets is analyzed in the present paper. Four different anisotropic plasticity models are used, i.e. the models suggested by Hill (1948, 1990), Barlat and Lian (1989) and Gotoh (1977). For all four models the yield surfaces and hardening behavior are fitted to agree with experimental results of Kuwabara et al. (1998a) for a cold-rolled steel sheet. The basic formulations for the rotation of the yield surface during deformation make use of models developed by Dafalias (1985, 1993) and Kuroda (1997). In all previous analyses of necking in anisotropic metal sheets, the principal tensile axes have been along the orthotropic axes of the

anisotropy, but here we focus also on tension in directions inclined to the initial orthotropic axes, so that a description of the rotation of the orthotropic axes with deformation is a necessary part of the analysis. In the localization studies two different sets of boundary conditions on the deformations outside the band are considered, which are both natural extensions of the standard boundary conditions used in M-K-model analyses.

2. Anisotropic plasticity models

2.1. Generalities

A framework of constitutive equations considered here is based on the one generalized by Dafalias (1985, 1993). Assuming a small elastic and finite plastic deformation, we can write the kinematics in the rate form,

$$\mathbf{D} = \mathbf{D}^{\mathrm{e}} + \mathbf{D}^{\mathrm{p}} = \mathbf{D}^{\mathrm{e}} + \langle\lambda\rangle\mathbf{N}^{\mathrm{p}} \tag{1}$$

$$\mathbf{W} = \boldsymbol{\omega} + \mathbf{W}^{\mathrm{p}} = \boldsymbol{\omega} + \langle\lambda\rangle\boldsymbol{\Omega}^{\mathrm{p}} \tag{2}$$

where $\mathbf{D}$ is the rate of deformation tensor (symmetric part of the velocity gradient tensor $\mathbf{L} = \partial v_i/\partial x_j \mathbf{e}_i \otimes \mathbf{e}_j$, where $\mathbf{v}$ is the velocity of a material particle, $\mathbf{x}$ is the current position and $\mathbf{e}_i$ the Cartesian basis), $\mathbf{W}$ is the continuum spin tensor (antisymmetric part of $\mathbf{L}$), the superscripts e and p denote the elastic and plastic parts, $\boldsymbol{\omega}$ is the spin of material substructure, and $\mathbf{N}^{\mathrm{p}}$ and $\boldsymbol{\Omega}^{\mathrm{p}}$ define the direction of $\mathbf{D}^{\mathrm{p}}$ and $\mathbf{W}^{\mathrm{p}}$, respectively. The scalar-valued quantity λ is a loading index which is determined by a consistency condition of yield function, and $\langle\ \rangle$ are the Macauley brackets defining the operation $\langle\lambda\rangle = \lambda$ if $\lambda > 0$ and $\langle\lambda\rangle = 0$ if $\lambda \leq 0$.

The state variables will be the Cauchy stress $\boldsymbol{\sigma}$ and a set $\mathbf{s}_i$ of structure variables consisting of second-order tensors $\mathbf{a}_i$ (here we consider symmetric tensors only), vectors $\mathbf{b}_i$, and scalars k_i. With the superposed ($^\circ$) denoting an objective rate with respect to the substructure spin $\boldsymbol{\omega}$, the evolution laws for state variables are assumed to be given by,

$$\mathring{\boldsymbol{\sigma}} = \dot{\boldsymbol{\sigma}} - \boldsymbol{\omega}\boldsymbol{\sigma} + \boldsymbol{\sigma}\boldsymbol{\omega} = \mathbf{C}{:}\mathbf{D}^{\mathrm{e}} = \mathbf{C}{:}\mathbf{D} - \langle\lambda\rangle\mathbf{C}{:}\mathbf{N}^{\mathrm{p}} \tag{3}$$

$$\mathring{\mathbf{s}}_i = \langle\lambda\rangle\bar{\mathbf{s}}_i(\boldsymbol{\sigma}, \mathbf{s}_i); \tag{4a}$$

$$\mathring{\mathbf{a}}_i = \dot{\mathbf{a}}_i - \boldsymbol{\omega}\mathbf{a}_i + \mathbf{a}_i\boldsymbol{\omega} = \langle\lambda\rangle\bar{\mathbf{a}}_i \tag{4b}$$

$$\mathring{\mathbf{b}}_i = \dot{\mathbf{b}}_i - \boldsymbol{\omega}\mathbf{b}_i = \langle\lambda\rangle\bar{\mathbf{b}}_i \tag{4c}$$

$$\mathring{k} = \dot{k} = \langle\lambda\rangle\bar{k} \tag{4d}$$

where $\mathbf{C}$ is a fourth order elastic moduli tensor. Eq. (1) has been used for the last expression of Eq. (3). If a structure variable does not have any contribution to plastic hardening, such as a purely orientational quantity indicating an anisotropic direction, we consider $\bar{\mathbf{a}}_i \equiv 0$ or $\bar{\mathbf{b}}_i \equiv 0$ regardless of the value of $\langle\lambda\rangle$.

The equation of a yield surface is defined by

$$f(\boldsymbol{\sigma}, \mathbf{s}_i) = 0 \tag{5}$$

where f is an isotropic function of $\boldsymbol{\sigma}$ and $\mathbf{s}_i$. The consistency condition for continuing plastic deformation is

$$\dot{f} = \frac{\partial f}{\partial \boldsymbol{\sigma}} : \dot{\boldsymbol{\sigma}} + \frac{\partial f}{\partial \mathbf{s}_i} : \dot{\mathbf{s}}_i = \frac{\partial f}{\partial \boldsymbol{\sigma}} : \mathring{\boldsymbol{\sigma}} + \frac{\partial f}{\partial \mathbf{s}_i} : \mathring{\mathbf{s}}_i = 0. \tag{6}$$

With the notation $\mathbf{N}^{\mathrm{n}} = \partial f / \partial \boldsymbol{\sigma}$, we obtain the relations for λ, using Eqs. (3) and (4a), as follows:

$$\lambda = \frac{\mathbf{N}^{\mathrm{n}} : \mathring{\sigma}}{H_0} = \frac{\mathbf{N}^{\mathrm{n}} : \mathbf{C} : \mathbf{D}}{H_0 + \mathbf{N}^{\mathrm{n}} : \mathbf{C} : \mathbf{N}^{\mathrm{p}}}; \quad H_0 = -\frac{\partial f}{\partial \mathbf{s}_i} : \bar{\mathbf{s}}_i \tag{7a,b}$$

Substituting the last expression of Eq. (7a) into (3), an elasto-plastic constitutive relation between $\mathring{\sigma}$ and $\mathbf{D}$ is derived as

$$\mathring{\boldsymbol{\sigma}} = \left[\mathbf{C} - \frac{(\mathbf{C} : \mathbf{N}^{\mathrm{p}}) \otimes (\mathbf{N}^{\mathrm{n}} : \mathbf{C})}{H_0 + \mathbf{N}^{\mathrm{n}} : \mathbf{C} : \mathbf{N}^{\mathrm{p}}} \right] : \mathbf{D} \tag{8}$$

Further, using Eq. (2), we can derive an expression for the constitutive relation in terms of the Jaumann stress rate, $\mathring{\boldsymbol{\sigma}}^{\mathrm{J}} = \dot{\boldsymbol{\sigma}} - \mathbf{W}\boldsymbol{\sigma} + \boldsymbol{\sigma}\mathbf{W}$, as follows,

$$\mathring{\boldsymbol{\sigma}}^{\mathrm{J}} = \left[\mathbf{C} - \frac{\left\{ \mathbf{C} : \mathbf{N}^{\mathrm{p}} - (\boldsymbol{\sigma}\boldsymbol{\Omega}^{\mathrm{p}} - \boldsymbol{\Omega}^{\mathrm{p}}\boldsymbol{\sigma}) \right\} \otimes (\mathbf{N}^{\mathrm{n}} : \mathbf{C})}{H_0 + \mathbf{N}^{\mathrm{n}} : \mathbf{C} : \mathbf{N}^{\mathrm{p}}} \right] : \mathbf{D} \equiv \bar{\mathbf{C}} : \mathbf{D} \tag{9}$$

In this study, only an isotropic and constant $\mathbf{C}$ is considered, which is determined by the Young's modulus E and the Poisson's ratio ν.

Since Dafalias (1983, 1985) first proposed a general formulation for the plastic spin, it has been actively applied to various types of plasticity models and problems so far. In the present investigation, the skew tensor $\boldsymbol{\Omega}^{\mathrm{p}}$ in Eq. (2) is assumed to be given by

$$\boldsymbol{\Omega}^{\mathrm{p}} = \beta(\boldsymbol{\sigma}\mathbf{N}^{\mathrm{p}} - \mathbf{N}^{\mathrm{p}}\boldsymbol{\sigma}); \qquad \beta = \frac{q}{\sigma_{\mathrm{eq}}} \tag{10}$$

where q is a plastic spin coefficient and σ_{eq} is a properly defined *equivalent* stress. In the previous study (Kuroda, 1997), it has been shown that Eq. (10) provides fairly reasonable predictions of change in orientation of anisotropy for large reversed shear deformations. Very recently, Dafalias (1998, 1999) has pointed out that Eq. (10) can also reproduce experimental observations for the orientational evolution of anisotropy during tensile deformations (Kim and Yin, 1997), according to a choice of values of the plastic spin coefficient. It is noted that Eq. (10) is interpreted as a particular case of a plastic spin formulation method based on weighted 'average' of structure variables including the stress σ, which was provided in the earlier paper of Dafalias (1983). In Ref. Dafalias (1998) it has been also mentioned that the plastic spin formulation, which is based on the direct use of the representation theorem for each structure variable, i.e. $\boldsymbol{\Omega}^{\mathrm{p}} = \eta_1(\mathbf{a}_1\boldsymbol{\sigma} - \boldsymbol{\sigma}\mathbf{a}_1) + \eta_2(\mathbf{a}_2\boldsymbol{\sigma} - \boldsymbol{\sigma}\mathbf{a}_2) + \eta_3(\mathbf{a}_1\boldsymbol{\sigma}\mathbf{a}_2 - \mathbf{a}_2\boldsymbol{\sigma}\mathbf{a}_1)$ with $\mathbf{a}_1 = \mathbf{n}_1 \otimes \mathbf{n}_1$ and $\mathbf{a}_2 = \mathbf{n}_2 \otimes \mathbf{n}_2$ (Dafalias, 1983, 1985; Dafalias and Rashid, 1989), hardly reproduces the aforementioned experimental observations for orientational evolution of anisotropy. Lee et al. (1995) investigated the effects of plastic spin on strain localization in orthotropic material represented by Hill's (1948) quadratic yield criterion. Since their plastic spin formulation corresponds to the latter one, their results cannot be directly compared with the results to be shown in the present paper.

2.2. Anisotropic plasticity with orthotropic symmetries

Our discussion is restricted to the anisotropy with orthotropic symmetries, and we consider four orthotropic yield functions: Hill's 1948 quadratic (Hill, 1948), Hill's 1990 non-integer powers (Hill, 1990), Barlat and Lian's arbitrary powers (Barlat and Lian, 1989) and Gotoh's biquadratic (Gotoh, 1977). The latter three yield functions were proposed for in-plane stress (sheet) analysis only.

We state first some common assumptions that will be introduced into the analyses. Throughout the present investigation, an associated flow rule, $\mathbf{N}^{\mathrm{p}} = \mathbf{N}^{\mathrm{n}} = \partial f/\partial \boldsymbol{\sigma}$, is adopted. The current orthotropic axes are specified by the orthonormal basis $\mathbf{n}_i$. The $\mathbf{n}_i$ are purely orientational quantities, so that we can set $\mathring{\mathbf{n}}_i \equiv \mathbf{0}$ and then we have the following equation for orientational evolution of orthotropy:

$$\dot{\mathbf{n}}_i = \boldsymbol{\omega}\mathbf{n}_i. \tag{11}$$

Eq. (11) corresponds to the general expression (4c).

The tensor components in reference to the orthonormal axes $\hat{x}_i$ (i.e. $\mathbf{n}_i$) are denoted by the superposed ($\hat{}$), e.g. $\boldsymbol{\sigma} = \sigma_{ij}\mathbf{e}_i \otimes \mathbf{e}_j = \hat{\sigma}_{ij}\mathbf{n}_i \otimes \mathbf{n}_j$, $\mathbf{N}^{\mathrm{p}} = N^{\mathrm{p}}_{ij}\mathbf{e}_i \otimes \mathbf{e}_j = \hat{N}^{\mathrm{p}}_{ij}\mathbf{n}_i \otimes \mathbf{n}_j$, etc., where $\mathbf{e}_i$ are the fixed Cartesian basis. Accordingly, we can calculate the components $\partial f/\partial \sigma_{ij}$ in reference to the fixed Cartesian coordinate system as

$$\frac{\partial f}{\partial \sigma_{ij}} = \frac{\partial f}{\partial \hat{\sigma}_{kl}}\frac{\partial \hat{\sigma}_{kl}}{\partial \sigma_{ij}}. \tag{12}$$

The rolling direction 'R.D.', transverse direction 'T.D.' and normal (thickness) direction 'N.D.' are chosen to coincide initially with the axes $\hat{x}_1$, $\hat{x}_2$ and $\hat{x}_3$, respectively. The uniaxial yield (or flow) stress in a tensile specimen for α° to R.D. is denoted by σ_α: for instance, σ_0, σ_{45}, etc., and their initial values are denoted by $\sigma^{\mathrm{I}}_\alpha$. The values of σ_α 's are assumed to be governed by a power-law function of an equivalent plastic strain ε^{p} as

$$\sigma_\alpha = \sigma^{\mathrm{I}}_\alpha\left(1 + \frac{\varepsilon^{\mathrm{p}}}{\varepsilon_0}\right)^n \tag{13}$$

where n is the strain hardening exponent, and ε_0 is a material constant. In addition to σ_α's, we define σ_{bi} the yield stress in equibiaxial tension: i.e. $\hat{\sigma}_{11} = \hat{\sigma}_{22} = \sigma_{\mathrm{bi}}$ for continuing plastic deformation under the equibiaxial tension, which is also governed by the same power-law function as Eq. (13). The r-values (the ratio of width to thickness strain rates) for the α direction are denoted by r_α. The r_α's are assumed to be constants throughout the present paper. Validity of this assumption will be discussed in Section 4. The orthotropic axis $\hat{x}_3$ is identical to the axis x_3 of the fixed Cartesian coordinate system throughout the analysis because a plane stress state is assumed, while the axes $\hat{x}_1$ and $\hat{x}_2$ may rotate relative to x_1 and x_2, according to Eq. (11). It is assumed that the material properties characterized by σ_α, σ_{bi} and r_α, which are determined in reference to the initial state of $\hat{x}_1$ and $\hat{x}_2$ (= R.D. and T.D., respectively), will be maintained for any rotated state of the $\hat{x}_1$ and $\hat{x}_2$ axes: i.e. the rotation of orthotropic axes does not affect the material properties observed on the orthotropic axes $\hat{x}_i$.

The rate of the equivalent plastic strain is defined simply by

$$\dot{\varepsilon}^{\mathrm{p}} = \sqrt{\frac{2}{3}\mathbf{D}^{\mathrm{p}}:\mathbf{D}^{\mathrm{p}}} = \langle\lambda\rangle\sqrt{\frac{2}{3}\mathbf{N}^{\mathrm{p}}:\mathbf{N}^{\mathrm{p}}}, \tag{14}$$

and the total equivalent strain is obtained from $\varepsilon^{\mathrm{p}} = \int \dot{\varepsilon}^{\mathrm{p}}\,\mathrm{d}t$. The last expression in Eq. (14) corresponds to the general expression (4d). It is noted that the use of the unified definition for $\dot{\varepsilon}^{\mathrm{p}}$ in Eq. (14) implies that we adopt here a simple 'strain-hardening' assumption, and do not use the 'work-hardening'

assumption based on an equivalency $\boldsymbol{\sigma}:\mathbf{D}^{\mathrm{p}} = \boldsymbol{\sigma}_{\mathrm{eq}}\dot{\varepsilon}^{\mathrm{p}}$. Advantages, as well as disadvantages, in both the assumptions of work-hardening and strain-hardening are still at issue.

2.2.1. Hill's (1948) quadratic

The most classical and familiar anisotropic yield criterion proposed by Hill (1948) is

$$f = \sqrt{\frac{3}{2(F+G+H)}}\left[(G+H)\hat{\sigma}_{11}^2 - 2H\hat{\sigma}_{11}\hat{\sigma}_{22} + (F+H)\hat{\sigma}_{22}^2 + 2N\hat{\sigma}_{12}^2\right]^{1/2} - C\sigma_0 = 0 \tag{15}$$

$$C = \sqrt{\frac{3(G+H)}{2(F+G+H)}} \tag{16}$$

where F, G, H and N are orthotropic coefficients which are determined by

$$\frac{G}{H} = \frac{1}{r_0}; \quad \frac{F}{H} = \frac{1}{r_{90}}; \quad \frac{N}{H} = \left(r_{45} + \frac{1}{2}\right)\left(\frac{1}{r_0} + \frac{1}{r_{90}}\right) \tag{17}$$

in a commonly used way. The orthotropic coefficients, of course, can be also determined with yield (flow) stresses obtained from uniaxial and equibiaxial tensile tests. Discussion of methods for determining the coefficients will be provided later. If we assume $F = G = H$ and $N = 3F$, Eq. (15) is reduced to the Mises criterion. The hardening modulus in the constitutive relation (8) or (9) is

$$H_0 = C\frac{\mathrm{d}\sigma_0}{\mathrm{d}\varepsilon^{\mathrm{p}}}\sqrt{\frac{2}{3}\mathbf{N}^{\mathrm{p}}:\mathbf{N}^{\mathrm{p}}}. \tag{18}$$

2.2.2. Hill's (1990) non-integer powers

Hill (1990) proposed the following yield criterion as an improvement of his 1948 quadratic one:

$$\begin{aligned} f = {} & \frac{1}{2}\Big[|\hat{\sigma}_{11} + \hat{\sigma}_{22}|^m + \left(\sigma_{\mathrm{bi}}^m/\tau^m\right)|(\hat{\sigma}_{11} - \hat{\sigma}_{22})^2 + 4\hat{\sigma}_{12}^2|^{m/2} + |\hat{\sigma}_{11}^2 + \hat{\sigma}_{22}^2 + 2\hat{\sigma}_{12}^2|^{m/2-1}\Big\{ - 2a\left(\hat{\sigma}_{11}^2 - \hat{\sigma}_{22}^2\right) \\ & + b(\hat{\sigma}_{11} - \hat{\sigma}_{22})^2\Big\}\Big]^{1/m} - \sigma_{\mathrm{bi}} \\ = {} & 0 \end{aligned} \tag{19}$$

$$\sigma_{\mathrm{bi}}^m/\tau^m = (2\sigma_{\mathrm{bi}}/\sigma_{45})^m - 1 \tag{20}$$

$$a = \frac{1}{4}\left\{(2\sigma_{\mathrm{bi}}/\sigma_{90})^m - (2\sigma_{\mathrm{bi}}/\sigma_0)^m\right\} \tag{21}$$

$$b = \frac{1}{2}\left\{(2\sigma_{\mathrm{bi}}/\sigma_0)^m + (2\sigma_{\mathrm{bi}}/\sigma_{90})^m\right\} - (2\sigma_{\mathrm{bi}}/\sigma_{45})^m \tag{22}$$

where $m > 1$. When $\sigma_{\mathrm{bi}} = \sigma_0 = \sigma_{45} = \sigma_{90}$ with $m = 2$, Eq. (19) is reduced to the Mises criterion. Based on the above yield function and Eq. (7b), we obtain the strain hardening modulus as follows:

$$H_0 = -\frac{\partial f}{\partial \varepsilon^p}\sqrt{\frac{2}{3}\mathbf{N}^p:\mathbf{N}^p} \tag{23}$$

where

$$\frac{\partial f}{\partial \varepsilon^p} = \frac{\partial f}{\partial \sigma_{bi}}\frac{d\sigma_{bi}}{d\varepsilon^p} + \frac{\partial f}{\partial \sigma_0}\frac{d\sigma_0}{d\varepsilon^p} + \frac{\partial f}{\partial \sigma_{90}}\frac{d\sigma_{90}}{d\varepsilon^p} + \frac{\partial f}{\partial \sigma_{45}}\frac{d\sigma_{45}}{d\varepsilon^p}. \tag{24}$$

2.2.3. Barlat and Lian's (1989) arbitrary powers

Motivated by earlier works by Hershey (1954), Hosford (1972), Hill (1979) and Logan and Hosford (1980), Barlat and Lian (1989) proposed the following yield criterion:

$$f = \left[\frac{1}{2}\left(a|K_1 + K_2|^M + a|K_1 - K_2|^M + c|2K_2|^M\right)\right]^{1/M} - \sigma_0 = 0 \tag{25}$$

$$K_1 = \frac{\hat{\sigma}_{11} + h\hat{\sigma}_{22}}{2}, \quad K_2 = \sqrt{\left(\frac{\hat{\sigma}_{11} - h\hat{\sigma}_{22}}{2}\right)^2 + p^2\hat{\sigma}_{12}^2} \tag{26a,b}$$

where a, c, h and p are orthotropic coefficients. If we assume that M is known, these coefficients can be determined with yield (flow) stresses obtained from uniaxial and equibiaxial tensile tests or r-values data. Although Barlat and Lian (1989) mainly considered to use the r-values data, we use here the tensile test data as in Hill's (1990) criterion, i.e.

$$a = 2 - c, \quad c = \frac{2\left\{\sigma_{bi}^M + (h\sigma_{bi})^M\right\} - 2\sigma_0^M}{\sigma_{bi}^M + (h\sigma_{bi})^M - |(1-h)\sigma_{bi}|^M}, \quad h = \frac{\sigma_0}{\sigma_{90}}. \tag{27a,b,c}$$

The coefficient p cannot be calculated analytically. However, after determining a, c and h, we can have a nonlinear algebraic equation for p by substituting $\hat{\sigma}_{11} = \hat{\sigma}_{22} = \hat{\sigma}_{12} = \frac{1}{2}\sigma_{45}$ into Eq. (25). Using this equation, the value of p can be found numerically. When $\sigma_{bi} = \sigma_0 = \sigma_{45} = \sigma_{90}$, i.e. $a = c = h = p = 1$ with $m = 2$, Eq. (25) is reduced to the Mises criterion. We obtain the strain hardening modulus by Eq. (23) with

$$\frac{\partial f}{\partial \varepsilon^p} = \left(\frac{\partial f}{\partial c} - \frac{\partial f}{\partial a}\right)\left(\frac{\partial c}{\partial \sigma_{bi}}\frac{d\sigma_{bi}}{d\varepsilon^p} + \frac{\partial c}{\partial \sigma_0}\frac{d\sigma_0}{d\varepsilon^p} + \frac{\partial c}{\partial h}\frac{dh}{d\varepsilon^p}\right) + \left(\frac{\partial f}{\partial K_1}\frac{\partial K_1}{\partial h} + \frac{\partial f}{\partial K_2}\frac{\partial K_2}{\partial h}\right)\frac{dh}{d\varepsilon^p} + \frac{\partial f}{\partial K_2}\frac{\partial K_2}{\partial p}\frac{dp}{d\varepsilon^p} - \frac{d\sigma_0}{d\varepsilon^p} \tag{28}$$

In the above equation, we cannot have analytical expression for $dp/d\varepsilon^p$ again. It is evaluated numerically.

Barlat and his co-workers (Barlat et al., 1991; 1997) subsequently proposed more generalized yield functions with six stress components, which could be potentially used for general three dimensional problems (but, the application has been restricted to sheet materials only). The yield criterion of Barlat et al. (1991) produced a plane stress yield surface that is very similar to the one predicted by Barlat and Lian's (1989) criterion in Eq. (25) as shown in Ref. Barlat et al. (1991). The last proposal by Barlat et al. (1997) includes Barlat and Lian's (1989) criterion (Eq. (25)) as a special case. In consideration of this, we employ the simpler yield criterion of Eq. (25) in this paper.

2.2.4. Gotoh's (1977) biquadratic

Motivated by Hill's suggestion (Hill, 1950), Gotoh (1977) proposed the following fourth order (biquadratic) yield criterion:

$$f = \Big[A_1\hat{\sigma}_{11}^4 + A_2\hat{\sigma}_{11}^3\hat{\sigma}_{22} + A_3\hat{\sigma}_{11}^2\hat{\sigma}_{22}^2 + A_4\hat{\sigma}_{11}\hat{\sigma}_{22}^3 + A_5\hat{\sigma}_{22}^4 + \Big(A_6\hat{\sigma}_{11}^2 + A_7\hat{\sigma}_{11}\hat{\sigma}_{22} + A_8\hat{\sigma}_{22}^2\Big)\hat{\sigma}_{12}^2 + A_9\hat{\sigma}_{12}^4\Big]^{1/4} - \sigma_0 = 0 \tag{29}$$

where

$$A_1 = 1, \quad A_2 = -\frac{4r_0}{1+r_0}, \quad A_4 = -\frac{4A_5 r_{90}}{1+r_{90}}, \tag{30a,b,c}$$

$$A_5 = (\sigma_0/\sigma_{90})^4, \qquad A_3 = (\sigma_{\mathrm{bi}}/\sigma_0)^{-4} - (A_1 + A_2 + A_4 + A_5) \tag{30d,e}$$

and $A_6 \sim A_9$ are determined with r_{45}, $r_{22.5}$, σ_{45} and $\sigma_{22.5}$, in addition to r_0, r_{90}, σ_0, σ_{90} and σ_{bi}. The detailed procedures for the determination of the remaining coefficients are given by Gotoh (1977). If all the σ_α 's, as well as σ_{bi}, are identical and all the r_α 's are equal to 1.0, Eq. (29) reduces to the Mises criterion. This isotropic condition is expressed in terms of the coefficients $A_1 \sim A_9$ as $A_2 = A_4 = -2A_1$, $A_3 = 3A_1$, $A_5 = A_1$, $A_6 = A_8 = -A_7 = 6A_1$ and $A_9 = 9A_1$ with $A_1 = 1$. The strain hardening modulus is given by

$$H_0 = -\frac{\partial f}{\partial \varepsilon^{\mathrm{p}}}\sqrt{\frac{2}{3}\mathbf{N}^{\mathrm{p}}:\mathbf{N}^{\mathrm{p}}} = \left(\frac{\mathrm{d}\sigma_0}{\mathrm{d}\varepsilon^{\mathrm{p}}} - \frac{\partial f}{\partial A_I}\frac{\mathrm{d}A_I}{\mathrm{d}\varepsilon^{\mathrm{p}}}\right)\sqrt{\frac{2}{3}\mathbf{N}^{\mathrm{p}}:\mathbf{N}^{\mathrm{p}}}. \tag{31}$$

2.2.5. Similarities and differences between the yield criteria

Special cases of the yield criteria, i.e. Hill's (1990) criterion with $m = 2$ and Barlat and Lian's (1989) criterion with $M = 2$, are completely identical. Moreover, the functional form of these is the same as the classical Hill's (1948) criterion. In this case, the difference of the above Hill's (1948) criterion to Hill's (1990) criterion with $m = 2$ (or Barlat and Lian's (1989) with $M = 2$) is only the method used to determine the orthotropic coefficients. As shown above, in Hill's (1948) quadratic criterion, we use only the r-value data. By contrast, in Hill's (1990) and Barlat and Lian's (1989) criteria, we use the yield stresses in uniaxial and biaxial tensile tests. Therefore, through a comparison of results for Hill's (1948) criterion to results for Hill's (1990) criterion with $m = 2$ (or Barlat and Lian's (1989) criterion with $M = 2$), we can observe rather small differences, resulting from the different methods for determining the coefficients. In the case of Gotoh's (1977) biquadratic, both the r-value data and yield (flow) stress data are used to determine the coefficients. In other words, Gotoh's (1977) biquadratic criterion accounts for both the effects of deformation anisotropy (r-values) and deformation resistance anisotropy (tensile yield stresses), although the power of stress in this yield criterion is fixed to four.

3. Sheet necking formulation

For the thin sheets considered here, with two of the orthotropic axes, $\hat{x}_1$ and $\hat{x}_2$, of the anisotropy in the plane of the sheet, in-plane stretching results in a plane stress state. Thus, with Greek letter

subscripts ranging from 1 to 2, representing in-plane quantities, the components L_{23}, L_{32}, L_{31} and L_{13} are automatically zero. From the plane stress requirement of zero stresses normal to the sheet, i.e. $\dot{\sigma}_{33} = 0$, we obtain a relationship between $L_{33}(= D_{33})$ and the in-plane components $D_{\alpha\beta}$. Using this, D_{33} can be eliminated from the 3D constitutive relation (9) as

$$\mathring{\sigma}^{\mathrm{J}}_{\alpha\beta} = \left[\bar{C}_{\alpha\beta\gamma\delta} - \frac{\bar{C}_{\alpha\beta 33}\bar{C}_{33\gamma\delta}}{\bar{C}_{3333}} \right] D_{\gamma\delta}. \tag{32}$$

All the yield criteria considered here are written in terms of the stress components $\hat{\sigma}_{11}$, $\hat{\sigma}_{22}$ and $\hat{\sigma}_{12}$ $(=\hat{\sigma}_{21})$, as shown in the previous section. They give directly $\partial f/\partial\sigma_{11}$, $\partial f/\partial\sigma_{22}$ and $\partial f/\partial\sigma_{12}$ with the use of Eq. (12). The component $\partial f/\partial\sigma_{33}$ is obtained from the plastic incompressibility assumption. Using these, we can calculate the components $\bar{C}_{ijkl}$ in Eq. (9) with respect to the fixed Cartesian coordinate system. Then, the components of the in-plane modulus are obtained from Eq. (32).

In the M–K-model it is assumed that a band of material contains an initial inhomogeneity, e.g. in the form of a reduced thickness of the sheet (see Fig. 1). The quantities inside the band are denoted by $(\,)^{\mathrm{b}}$ and the initial normal of the band is $\mathbf{m}^{\mathrm{I}} = (\cos\psi_{\mathrm{I}}, \sin\psi_{\mathrm{I}})$. Since uniform deformation fields are assumed both inside and outside the band, equilibrium and compatibility inside these two regions are automatically satisfied, apart from the necessary conditions along the edge of the band. These conditions are

$$F^{\mathrm{b}}_{\alpha\beta} = F_{\alpha\beta} + d_\alpha m^{\mathrm{I}}_\beta \tag{33}$$

$$m^{\mathrm{I}}_\alpha \Pi^{\mathrm{b}}_{\alpha\beta} h^{\mathrm{b}}_{\mathrm{I}} = m^{\mathrm{I}}_\alpha \boldsymbol{\Pi}_{\alpha\beta} h_{\mathrm{I}} \tag{34}$$

where $F_{\alpha\beta}$ are the components of the deformation gradient, h_{I} are the initial thicknesses, $\Pi_{\alpha\beta}$ are the components of the nominal stress $\boldsymbol{\Pi}$, and d_α are parameters to be determined. Thus, in the absence of

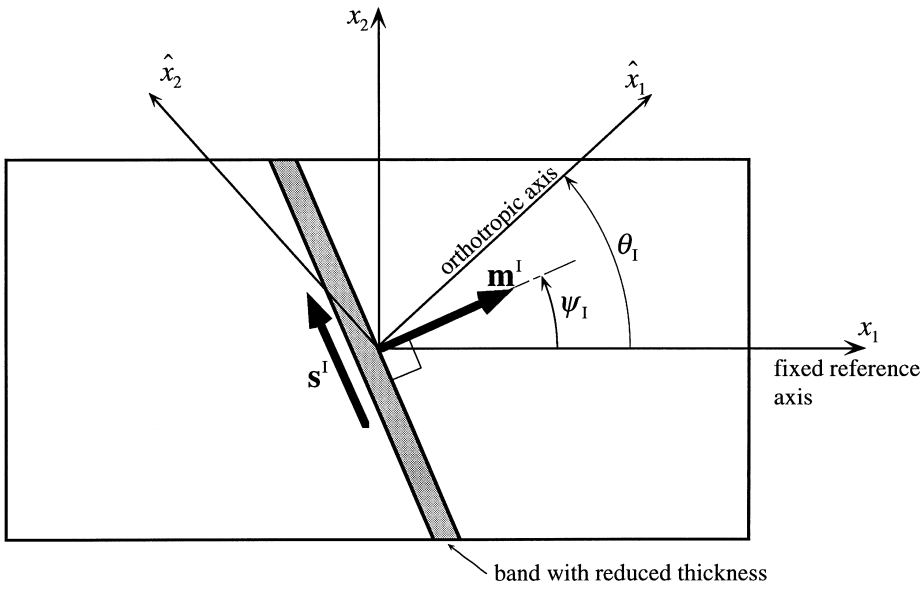

Fig. 1. Anisotropic thin sheet with an initial thickness imperfection initially inclined at an angle ψ_{I}.

material inhomogeneities, the initial imperfection is specified by the ratio $h_{\mathrm{I}}^{\mathrm{b}}/h_{\mathrm{I}}$. These equations determine the neck development for any prescribed history of the in-plane deformation gradients $F_{\alpha\beta}$ outside the band. Plastic flow localization is said to occur when straining stops outside the band (elastic unloading), while plastic straining continues inside the band.

In the present study an Eulerian version of Eqs. (33) and (34) is used. Thus, the compatibility condition at the band interface is given in terms of the differences between the velocity gradients inside and outside the band,

$$L_{\alpha\beta}^{\mathrm{b}} = L_{\alpha\beta} + \dot{c}_{\alpha} m_{\beta} \tag{35}$$

where $\dot{c}_{\alpha}$ are the parameters to be determined, and m_{β} are the components of the current unit normal $\mathbf{m}$ to the band, which is given by $\mathbf{m} = (\cos\psi,\ \sin\psi)$ in terms of the current angle ψ of the band. The Eulerian form of the equilibrium conditions at the band interface is

$$m_{\alpha}\sigma_{\alpha\beta}^{\mathrm{b}} h^{\mathrm{b}} = m_{\alpha}\sigma_{\alpha\beta} h. \tag{36}$$

Substituting the constitutive relation (in the plane stress form (32)) into the rate form of Eq. (36), with elimination of $L_{\alpha\beta}^{\mathrm{b}}$ using Eq. (35), gives simple algebraic equations having only two unknowns, $\dot{c}_1$ and $\dot{c}_2$. Once $\dot{c}_1$ and $\dot{c}_2$ are solved, we can calculate all the rate values of the variables to be updated.

For the deformations outside the band most M–K-analyses have assumed a constant ratio ρ of the logarithmic strains along the fixed Cartesian coordinate axes, with no shear straining. Then, the in-plane normal components of the velocity gradient are prescribed as follows:

$$\frac{L_{22}}{L_{11}} = \frac{D_{22}}{D_{11}} \equiv \frac{\dot{\varepsilon}_{22}}{\dot{\varepsilon}_{11}} = \rho = \text{constant}. \tag{37}$$

with the remaining components set to be

$$L_{12} = L_{21} = D_{12} = W_{21} = 0. \tag{38}$$

In this case, the current orientation of the band, ψ, is simply given by

$$\tan\psi = \exp\big[(1-\rho)\varepsilon_{11}\big]\tan\psi_{\mathrm{I}}. \tag{39}$$

In the case of standard isotropic hardening or kinematic hardening solids, the conditions (37) and (38) will automatically result in zero shear stress, $\sigma_{12} = 0$, outside the band. The same is true for anisotropic plasticity if the orthotropic axes of the anisotropy are in the fixed coordinate directions, i.e. if θ_{I} is set to be 0° or 90°, where θ_{I} is the initial orthotropic angle defined in Fig. 1. However, in many of the anisotropic cases to be analyzed here θ_{I} differs from 0° or 90°, and then the conditions (38) can result in the development of nonzero values of σ_{12} outside the band. For a few of these cases comparison will be made with analyses where Eq. (38) is replaced by the conditions

$$L_{12} \neq 0, \quad L_{21} = 0, \quad \sigma_{12} = 0. \tag{40}$$

These alternative conditions mean that, outside the band, material lines initially parallel to the x_1 axis will not rotate, but lines initially parallel to the x_2 axis may rotate, so that nonzero shear strains will develop, while the shear stress remains zero. In this case, the current unit normal vector $\mathbf{m}$ of the band can be obtained by the following more generalized way:

$$\mathbf{m} = \frac{1}{\sqrt{s_1^2 + s_2^2}} \begin{pmatrix} s_2 \\ -s_1 \end{pmatrix} \tag{41}$$

$$s_1 = F_{11} s_1^{\mathrm{I}} + F_{12} s_2^{\mathrm{I}}, \qquad s_2 = F_{21} s_1^{\mathrm{I}} + F_{22} s_2^{\mathrm{I}} \tag{42}$$

where s_β^{I} are the components of the initial tangential vector $\mathbf{s}^{\mathrm{I}}$ of the band. Eq. (39) is, of course, a special case of Eq. (41).

It is emphasized that, for the standard isotropic material, or for anisotropic materials with the orthotropic axes along the fixed coordinate axes, identical results are obtained by prescribing either the conditions (37) and (38) or the conditions (37) and (40), outside the band.

For the case of $h_{\mathrm{I}}^{\mathrm{b}}/h_{\mathrm{I}} < 1$, the onset of the sheet necking (localization), as defined above, is calculated as the occurrence of a much higher maximum principal logarithmic strain rate inside the band than outside the band, i.e. $\dot{\varepsilon}_1^{\mathrm{b}} \gg \dot{\varepsilon}_1$, where $\dot{\varepsilon}_1^{\mathrm{b}}$ and $\dot{\varepsilon}_1$ are the maximum principal values of the stretching tensors $\boldsymbol{D}^{\mathrm{b}}$ and $\mathbf{D}$, respectively. For the case of $h_{\mathrm{I}}^{\mathrm{b}}/h_{\mathrm{I}} = 1$ (no imperfection case), the problem becomes a bifurcation problem in which a bifurcation (the onset of the sheet necking) corresponds to the point where the determinant of the coefficient matrix of the algebraic equation for $\dot{c}_1$ and $\dot{c}_2$ becomes zero.

The strains $\varepsilon_{11}^{\mathrm{L}}$ and $\varepsilon_{22}^{\mathrm{L}}$ outside the band corresponding to the onset of the sheet necking are the *localization strains*. In the case of the conditions (37) and (38), ε_{11} and ε_{22} are the precise logarithmic principal strains. By contrast, in the case of the conditions (37) and (40), ε_{11} and ε_{22} are not precise logarithmic strain components, nor principal strains when the shear strain evolves outside the band. In this case, the strains to be shown in the results are calculated as $\varepsilon_{11} = \int D_{11}\,\mathrm{d}t$ and $\varepsilon_{22} = \rho\varepsilon_{11}$. They are used only as deformation measures for the purpose of comparison with the case of the conditions (37) and (38).

A point on one of the forming limit diagrams (FLD's) to be shown in the following section is obtained as follows: (i) calculating the localization strains, $\varepsilon_{11}^{\mathrm{L}}$ and $\varepsilon_{22}^{\mathrm{L}}$, for various values of the initial band angle ψ_{I}, (ii) finding the minimum value of the major localization strain $\varepsilon_{11}^{\mathrm{L}}$, and (iii) defining the minimum value of $\varepsilon_{11}^{\mathrm{L}}$ and the corresponding $\varepsilon_{22}^{\mathrm{L}}$ as the predicted *forming limit strains*, ε_{11}^{*} and ε_{22}^{*}, to be plotted on a FLD. The initial band angle corresponding to ε_{11}^{*} and ε_{22}^{*} is defined as the critical initial band angle ψ_{I}^{*}. A whole forming limit diagram is obtained by repeating the same procedure for various values of the strain rate ratio ρ. In the present study, it is assumed that the initial orthotropic angle θ_{I} ranges from 0° to 90°. Corresponding to this, we consider the values of ψ_{I} ranging from 0° to 90° for the cases of θ_{I} equal to 0° or 90°, and from -90° to 90° for the cases of θ_{I} being values other than 0° or 90°.

4. Results

4.1. Material properties

The material considered in the present analyses is a cold-rolled low-carbon steel sheet (Kuwabara et al., 1998a). Hardening characteristics and r-values assumed here are shown in Table 1. All the values of material parameters for σ_α and the r_α values were estimated by Kuwabara et al. (1998a). The r-values are considered as material constants according to the findings that these were not so sensitive to an increase in plastic strain, at least within 10% strains (Kuwabara et al., 1998b). Although these parameter values were estimated referring to the experimental data within 5% plastic strain, we will use the same values as an extrapolation beyond this plastic strain range. For Hill's (1990) criterion, the value of m is assumed to be 2.2 on the basis of a suggestion in Ref. Kuwabara et al. (1998a). For Barlat

Table 1
Hardening characteristics of cold-rolled low carbon steel

Tests	σ_α^1 (MPa)	ε_0	n	r_α
Uniaxial $\alpha = 0^\circ$	165	0.0041	0.209	2.01
$\alpha = 22.5^\circ$	167	0.0048	0.218	1.89
$\alpha = 45^\circ$	174	0.0044	0.203	1.52
$\alpha = 90^\circ$	170	0.0040	0.192	2.42
Equibiaxial	165	0.0040	0.260	–

and Lian's (1989) criterion, $M = 6$ is selected following the work of Logan and Hosford (1980) which was a basis of Barlat and Lian's (1989) criterion. Fig. 2 shows shapes of yield surfaces for two strain levels under biaxial tension, with the Mises yield surface included as reference at both strain levels. Only the yield surface shape according to Hill's (1948) criterion does not change with increasing plastic strain, because it has been determined by the constant r-values. The shapes of the other three yield surfaces change with increasing plastic deformation due to the different hardening characteristics of σ_0, σ_{90} and σ_{bi}. It is clear that at the initial shapes of these three yield surfaces would be very similar to the Mises yield surface (although the initial surfaces are not shown here), because the initial yield stresses, σ_0^I, σ_{90}^I and σ_{bi}^I, are almost the same with each other as shown in Table 1. It can be seen from Fig. 2 that for $\varepsilon^p = 0.03$ the deformed yield surface shapes according to the different criteria are close to each other, except for Hill's (1948) criterion determined with the constant r-values. At the larger strain level ($\varepsilon^p = 0.3$), the yield surfaces for Hill's (1990), Barlat and Lian's (1989) and Gotoh's (1977) criteria evolve differently. Here, Hill's (1948) criterion, which does not change its shape, has come almost within the differences between the other three criteria.

In the following calculations, the elastic constants are assumed to be $E = 206$ GPa and $\nu = 0.3$.

4.2. Difference between predictions based on the four yield criteria

Fig. 3 shows FLD's for the different yield criteria, when the initial orthotropic axes coincide with the reference Cartesian axes, i.e. $\theta_I = 0^\circ$. The plastic spin coefficient q in Eq. (10) is set to be zero for all the calculations shown in Fig. 3. The effect of the plastic spin will be shown and discussed later. The value

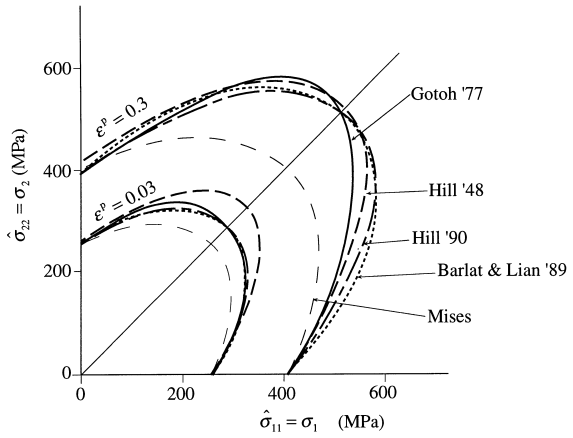

Fig. 2. Comparison of shapes of yield surfaces at small and large strain levels.

of the imperfection, h_I^b/h_I, is assumed to be 0.999 in most of the calculations. This value of the imperfection is considered to be in a realistic range and not too large compared to real metal products (Azrin and Backofen, 1970). For Hill's (1990) criterion, results for other values of h_I^b/h_I are included in Fig. 3, in order to illustrate the strong sensitivity to the imperfection level for $\rho > 0$. The bifurcation analysis ($h_I^b/h_I = 1$) does not give any realistic result in the biaxial stretching range (i.e. $\rho > 0$) as already known (e.g. Tvergaard, 1980).

The trends of FLD's for Hill's (1990) and Barlat and Lian's (1989) criteria are similar in Fig. 3, while the FLD for Gotoh's (1977) criterion shows a significant fall of the curve near the equibiaxial range. In the result for Hill's (1948) criterion, a very little fall of the curve can be seen too, near $\rho = 1$. The trend of a fall of FLD's near the equibiaxial stretching range has also been observed in some recent crystal plasticity predictions (Wu et al., 1997, 1998). It is also noted that if we continue to draw the FLD's beyond $\rho = 1$, i.e. for the range of $\rho > 1$, in Fig. 3, they will be asymmetric about the line of $\rho = 1$, unlike isotropic cases. We will see later FLD's corresponding to this range as those for $\rho < 1$ with $\theta_I = 90^\circ$ in Fig. 5.

Fig. 4(a) shows the relationships between the predicted critical initial band orientation, ψ_I^*, and the imposed ratio of strain rate, ρ, corresponding to Fig. 3. The trend of the ρ vs. ψ_I^* relation predicted by Gotoh's (1977) criterion, which shows a deviation of ψ_I^* from 0° in the range of $0.8 < \rho < 1$, is similar to the trend predicted by a crystal plasticity analysis (Wu et al., 1997; 1998). The ψ_I^* for Hill's (1948) criterion shows a sudden jump from 0° to 90°. This behavior is explained in Fig. 4(b), where curves of the localization strain ε_{11}^L versus the assumed initial band angle ψ_I for Gotoh's (1977) and for Hill's (1948) criteria are shown at nearly equibiaxial stretching, i.e. at $\rho = 0.9$ and 1.0. It is seen from the figure that in the case of Gotoh's (1977) criterion the bottom (i.e. $[\psi_I^*, \varepsilon_{11}^*]$,) of the curve (indicated by circles) gradually moves to the final point $[\psi_I^*, \varepsilon_{11}^*] = [70^\circ, 0.399]$ for $\rho = 1.0$. On the other hand, in the case of Hill's (1948) criterion, there are two bottoms at $\psi_I = 0^\circ$ and at 90°, and their locations on the ψ_I axis do not change. At some point in between $\rho = 0.9$ and 1.0, the minimum value of ε_{11}^L (i.e. ε_{11}^*) jumped from the bottom at $\psi_I = 0^\circ$ to the bottom at $\psi_I = 90^\circ$. Trends of curves of ε_{11}^L versus ψ_I for the other two yield criteria are similar to that for Hill's (1948) criterion. But, jumping the point of the minimum value of ε_{11}^L from $\psi_I = 0^\circ$ to 90° does not occur, i.e. the location of ε_{11}^* are fixed at $\psi_I = 0^\circ$

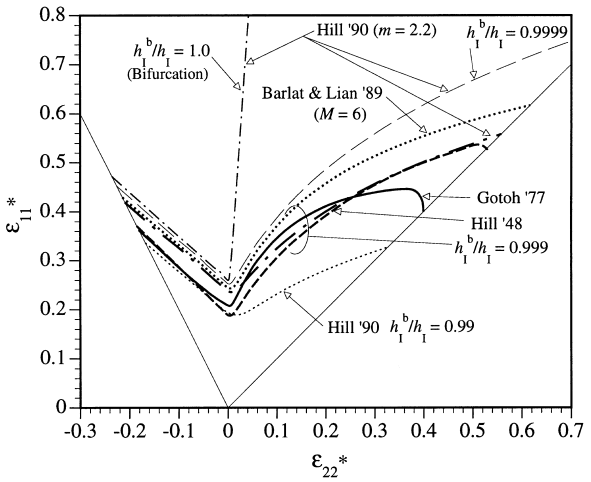

Fig. 3. Forming limit diagrams for four different yield criteria. The initial orthotropic axes coincide with the reference Cartesian coordinate system, i.e. $\theta_I = 0^\circ$.

until $\rho = 1.0$. It is noted that if isotropy is assumed the value of ε_{11}^{L} at $\rho = 1.0$ is identical for all values of ψ_I.

4.3. Effect of initial orientation of anisotropy

Fig. 5(a)–(d) show the effect of the initial orthotropic orientation, θ_I, on FLD's for the four different yield criteria. The boundary conditions (37) and (38) have been employed, i.e. $L_{12} = 0$. The plastic spin coefficient q is set to be zero again. The value of the geometrical imperfection, h_I^b/h_I, is assumed to be 0.999, and hereafter we will use this imperfection value only. The effect of the initial orthotropic

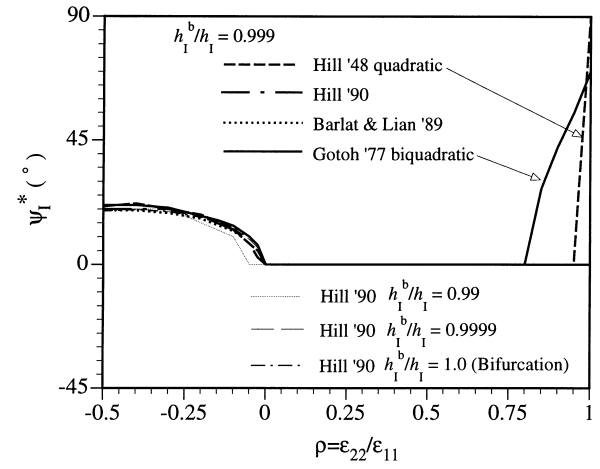

(a)

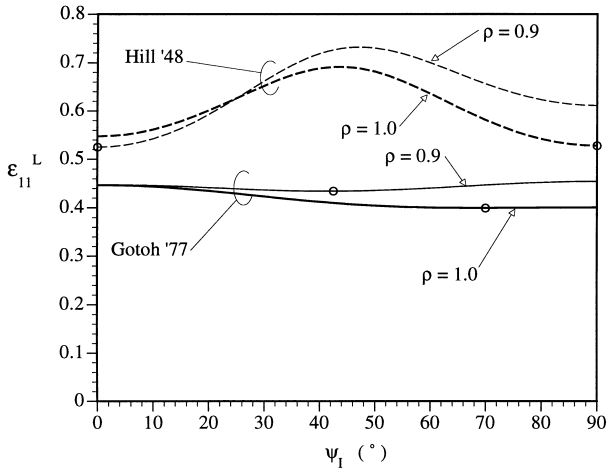

(b)

Fig. 4. Variation of critical initial band orientation ψ_I^* with ratio ρ of principal strains, corresponding to Fig. 3. (a) Critical band orientation ψ_I^* versus ratio ρ of principal strains. (b) Localization strain ε_{11}^{L} versus initial band orientation ψ_I near biaxial stretching; circles indicate critical points.

orientation on the predicted FLD differs much depending on the yield criterion employed, although all four yield criteria are obtained by fitting the same set of tensile test data. In the cases of Hill's (1948) and Barlat and Lian's (1989) criteria, the FLD's for $\theta_I = 0^\circ$ and 90° are very close to each other. On the other hand, the corresponding curves differ much in the cases of Hill's (1990) and Gotoh's (1977) criteria. It is noted that in the case of Hill's (1990) criterion, the limit strains for $\theta_I = 90^\circ$ are much higher than those for $\theta_I = 0^\circ$ in part of the range of $\rho > 0$, while a quite opposite tendency is observed for Gotoh's (1977) criterion. This can be attributed to the local curvature of the yield surface. For example, in the case of Gotoh's (1977) criterion, the yield surface curvature for the range of $\hat{\sigma}_{22} > \hat{\sigma}_{11}$ is much greater than that for $\hat{\sigma}_{11} > \hat{\sigma}_{22}$ (Fig. 2). It is expected that this large curvature region plays a role similar to that of a rounded vertex (Tvergaard, 1978) when $\theta_I = 90^\circ$ and $\rho > 0$. It is interesting to note that the results for Gotoh's (1977) criterion shown in Fig. 5(d) are very similar to results in Ref. Hoferlin et al. (1998) for a low carbon mild steel, which were predicted with a texture- and

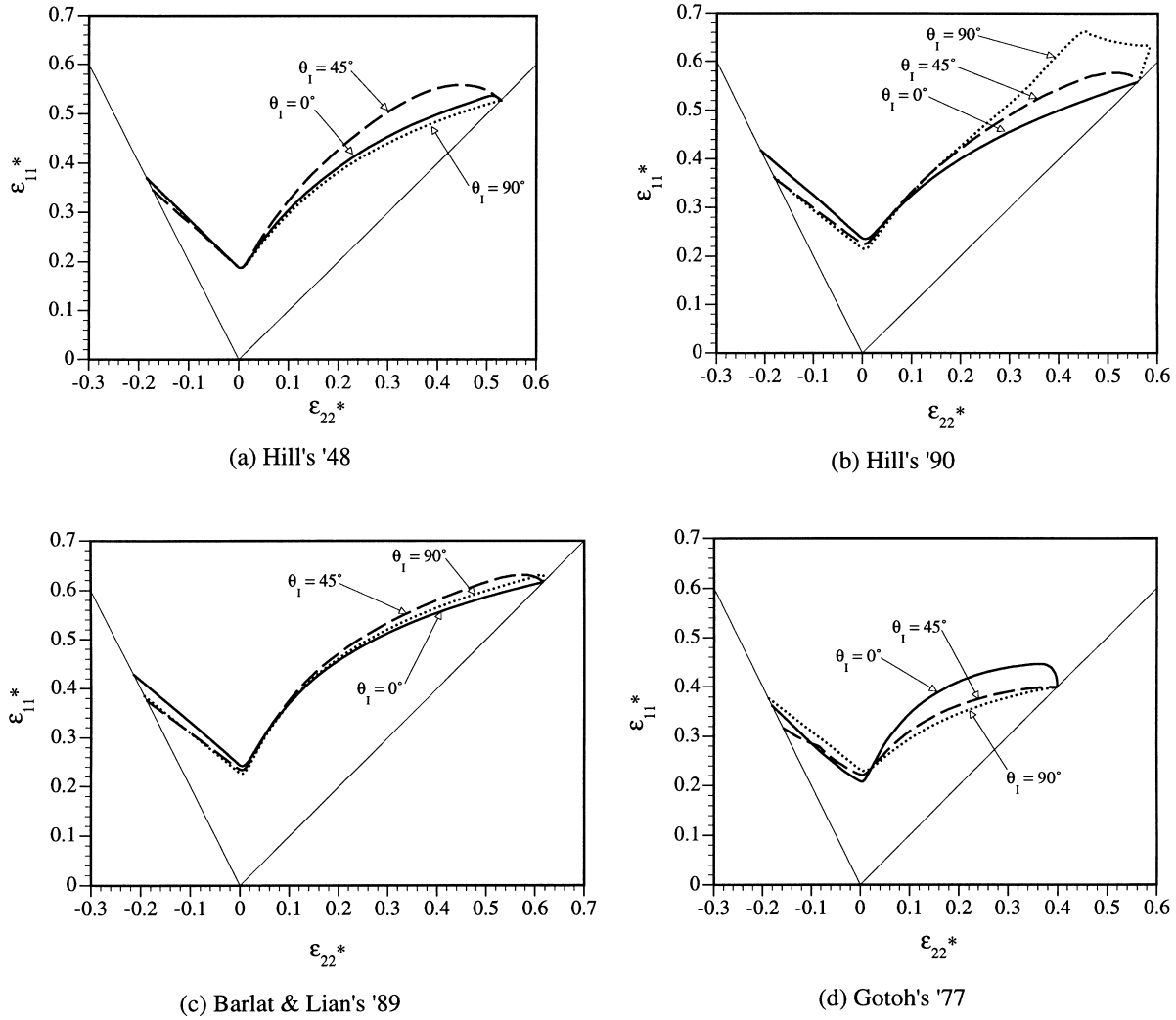

Fig. 5. Forming limit diagrams for three different initial orthotropic orientations; $h_I^b/h_I = 0.999$.

microstructure-based constitutive model. In their model, the shape of yield surface was generated on the basis of experimental crystallographic texture.

Consider in Fig. 5 the curves for $\theta_I = 0^\circ$ and 90° in the vicinity of the line $\rho = 1$. If the curve for $\theta_I = 0^\circ$ is followed up to $\rho = 1$, then continuation of this curve for values $\rho > 1$ corresponds to following the curve for $\theta_I = 90^\circ$ backwards with ρ decaying from the value one. This behavior is indicated most clearly in Fig. 5(b) and (d), by the angle of incidence of the two curves with the line $\rho = 1$.

Fig. 6(a) shows the FLD's for $\theta_I = 45^\circ$ for the four yield criteria, collected from Fig. 5(a)–(d). The corresponding critical initial band orientation, ψ_I^*, vs. the imposed ratio of strain rate, ρ, are depicted in Fig. 6(b). Different trends of the ψ_I^* vs. ρ relation are observed depending on the yield criterion. In particular, we notice a jump of ψ_I^* from -20° to $+20^\circ$ at $\rho = -0.3$ for Gotoh's criterion and large deviations of ψ_I^* from 0° in the range of $\rho > 0.2$ for all the criteria.

4.4. Effects of allowance of shear strain outside the imperfection band

Fig. 7(a)–(d) show FLD's for the two different types of boundary conditions mentioned in Section 3, i.e. for the conditions (37) combined with either Eqs. (38) or (40). Only for Gotoh's (1977) yield criterion, results for three values, 22.5°, 45° and 67.5°, of the initial orthotropic angle θ_I are depicted. For the other three yield criteria, only results for $\theta_I = 45^\circ$ are shown. The forming limit strains ε_{11}^* and ε_{22}^* are noticeably reduced by allowing of shear deformations along the x_1-axis (i.e. $L_{12} \neq 0$), especially in the range of $\rho > 0$. A similar effect of the two types of boundary condition has been seen for all the yield criteria, although the difference is not equally pronounced in the four cases. The smallest difference is found in Fig. 7(b), for Hill's (1990) criterion, while Gotoh's (1977) criterion in Fig. 7(c) shows the largest difference. In the case of $\theta_I = 0^\circ$ or 90°, the two sets of boundary conditions produce identical results due to orthotropic symmetries, as mentioned earlier.

4.5. Effects of plastic spin

The significance of the plastic spin concept in phenomenological plasticity theories for large strain

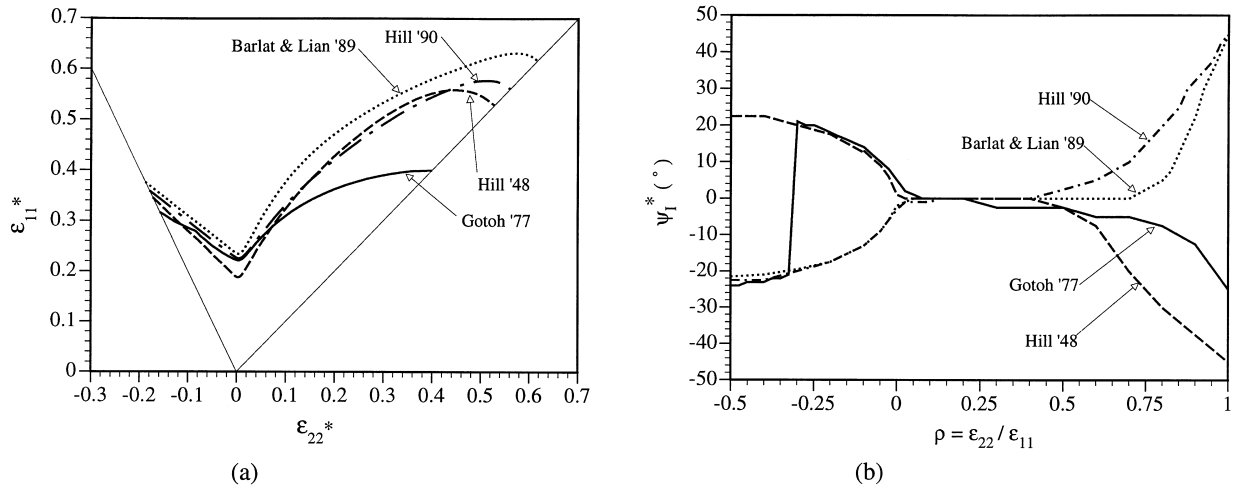

Fig. 6. (a) Forming limit diagrams for four different yield criteria; $\theta_I = 45^\circ$; $h_I^b/h_I = 0.999$. (b) critical band orientation ψ_I^* versus ratio ρ of principal strains (corresponding to (a)).

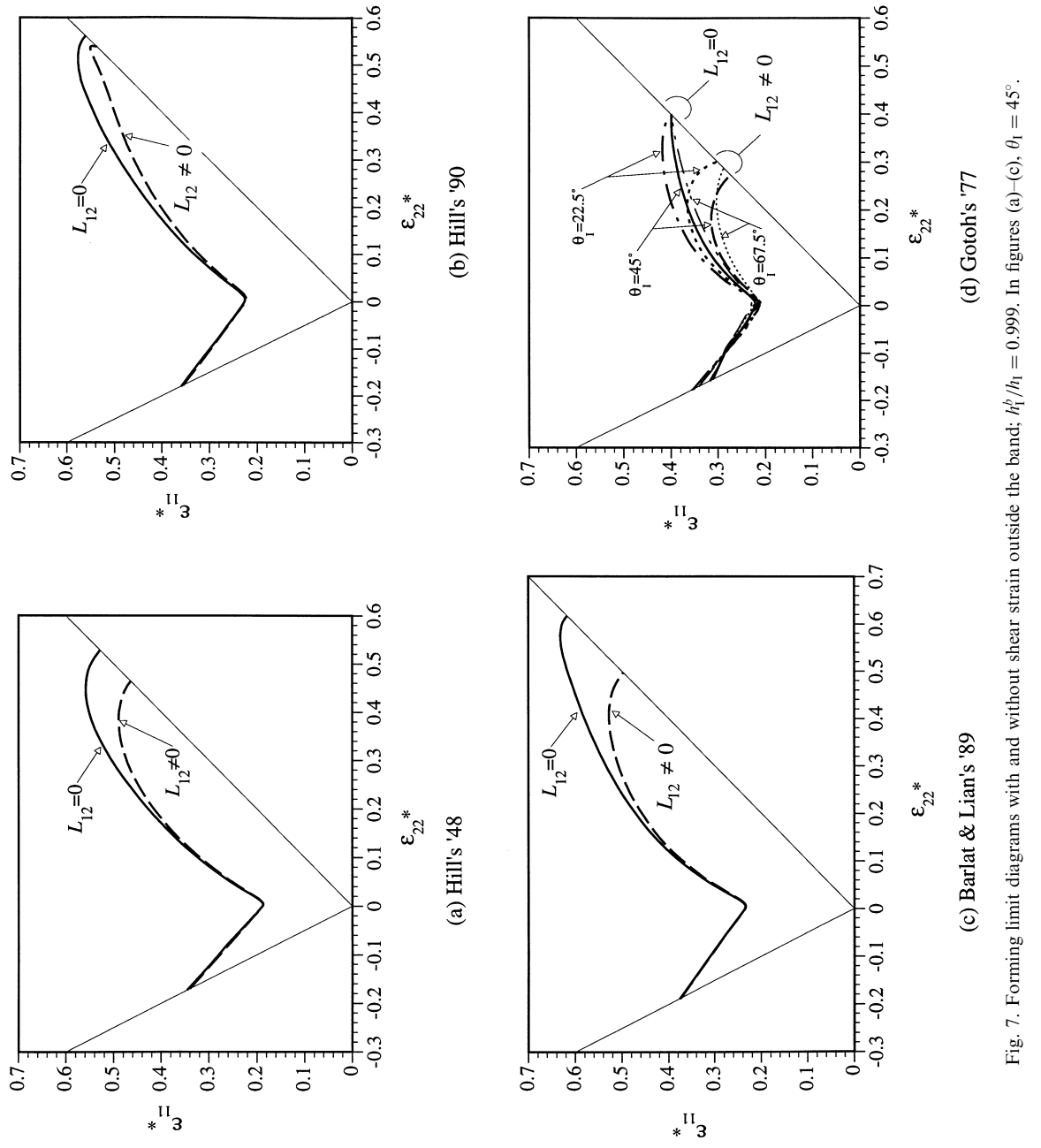

Fig. 7. Forming limit diagrams with and without shear strain outside the band; $h_I^b/h_I = 0.999$. In figures (a)–(c), $\theta_I = 45°$.

state has been widely recognized recently. When we adopt the plastic spin concept, two critical issues usually arise as: (i) how to choose a functional form of the plastic spin from many mathematical possibilities, and (ii) how to determine the coefficient(s) included in the formulation. Very recently, Dafalias (1998) pointed out that Eq. (10) has a fairly good potential to reproduce rather complicated experimental observations for significant changes in orientation of anisotropy during tensile deformations (Kim and Yin, 1997). In particular, he explained the different sense of rotation of anisotropy observed in the experiments for different directions of tension, as being related to the different sign of the shear strain rate component in reference to the principal stress axes, as derived by writing Eq. (10) in component form on these axes, and using Hill's (1948) quadratic yield criterion to compute $\mathbf{D}^{\mathrm{p}}$. In Kim and Yin's study, a cold rolled low carbon steel sheet was used, which is the same kind of steel sheets also considered in the present paper. In a comparison with their experimental results, Dafalias (1999) and we independently have found that the value $q = -100$ gives a good reproduction of

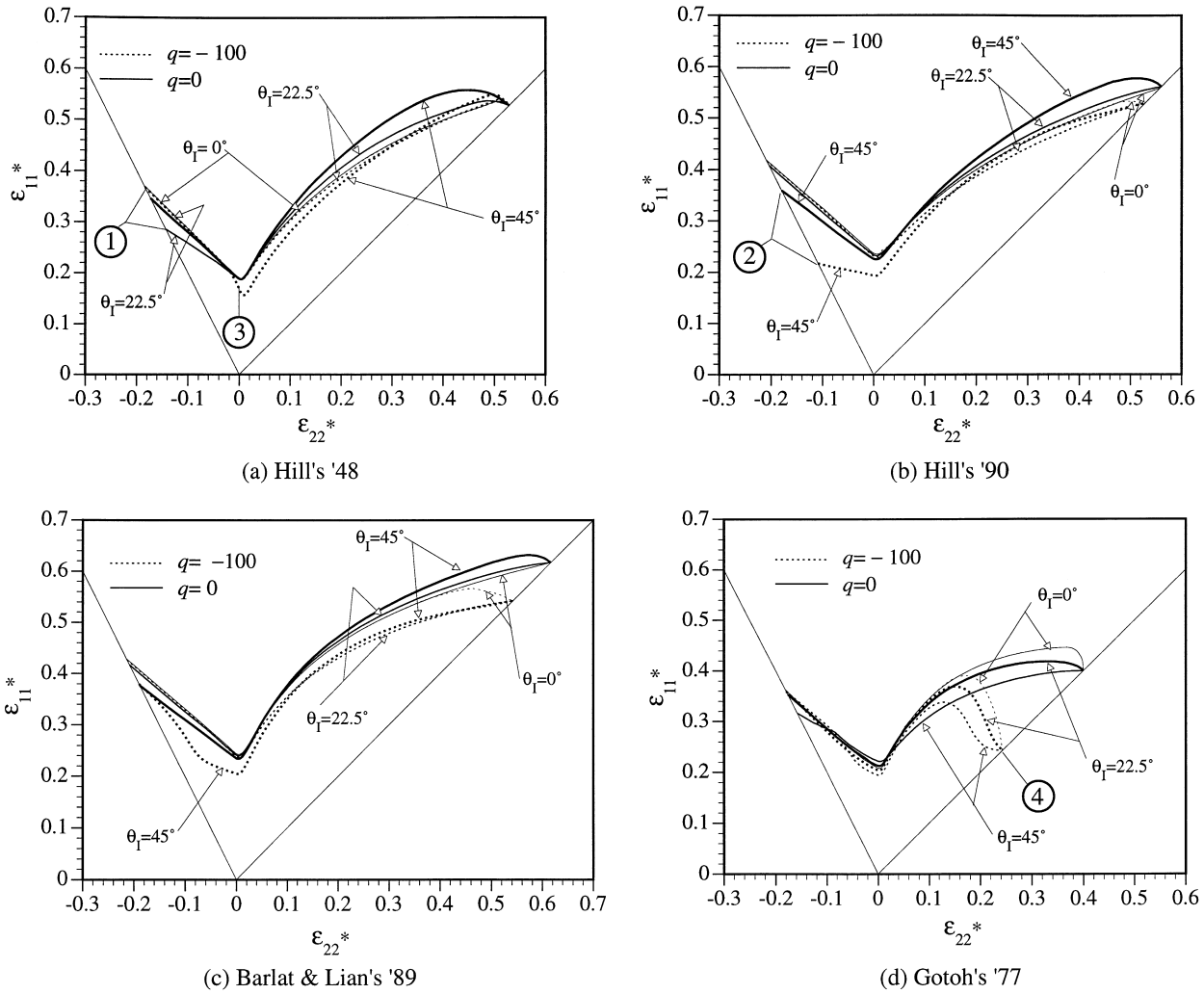

Fig. 8. Effect of plastic spin on FLD's; $h_{\mathrm{I}}^{b}/h_{\mathrm{I}} = 0.999$; $L_{12} = 0$ outside the band.

one of the experimental results in Ref. Kim and Yin (1997) when we adopt Hill's (1948) quadratic yield criterion. On the basis of these findings, we take here the value of q as -100, and make a comparison with predictions of the four yield criteria (even though the value $q = -100$ was found only for one of the criteria).

Fig. 8(a)–(d) show the effects of the plastic spin on FLD's for the four yield criteria. Results for three orthotropic orientations, $\theta_I = 0^\circ$, 22.5° and 45°, with two values of the plastic spin coefficient, $q = 0$ (no plastic spin) or $q = -100$ (the aforementioned value), are shown in each figure. The equivalent stress σ_{eq} in (10) is taken as $C\sigma_0$, σ_{bi}, σ_0 and σ_0, respectively, for Hill's (1948, 1990), Barlat and Lian's (1989) and Gotoh's (1977) criteria. The boundary conditions specified by Eqs. (37) and (38), i.e. $L_{12} = 0$, have been employed (no shear strain outside the band). In the case of Hill's (1948) criterion with $\theta_I = 0^\circ$, the difference between the results for $q = 0$ and -100 are invisible. It is observed that the plastic spin mainly reduces the limit strains in the range of $\rho > 0$, except for $0 < \rho < 0.4$ for Gotoh's (1977) criterion with $\theta_I = 22.5^\circ$ or 45° and for Hill's (1948) criterion with $\theta_I = 0^\circ$. Here, our attention is focused on the portions where the significant effects of plastic spin are observed. The typical portions are indicated by the encircled numbers in Fig. 8. Fig. 9(a)–(c) show the evolution of the orthotropic orientations outside and inside the band, θ and θ^b, with increasing principal logarithmic strain ε_{11}, for the portions indicated by the encircled numbers in Fig. 8. In the case of ① (Hill's (1948) with $\theta_I = 22.5^\circ$, $\rho = -0.5$), when the plastic spin ($q = -100$) is assumed, the orthotropic orientation θ rather quickly changes from the initial value ($=22.5^\circ$) to zero. This means that the orthotropic axis $\hat{x}_1$ tends to rotate towards the principal

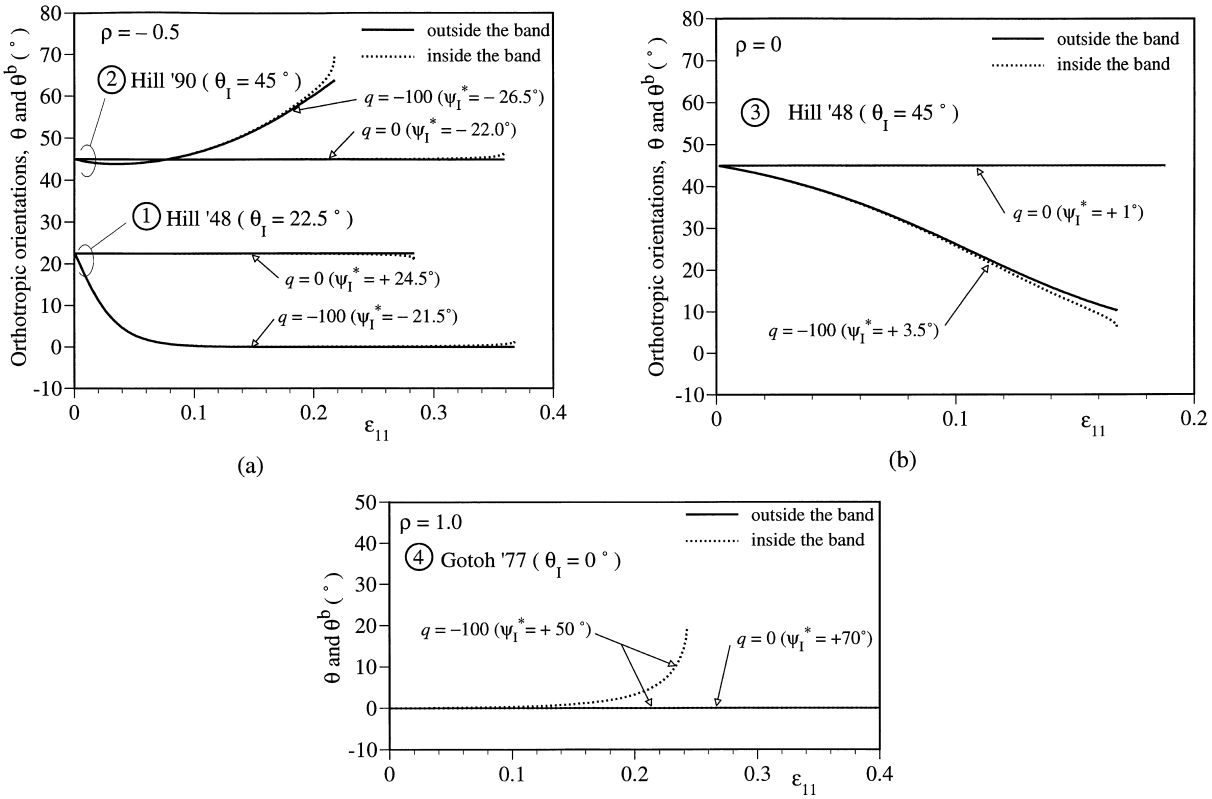

Fig. 9. Relationships between principal strain ε_{11} and orthotropic orientations θ inside and outside the band for particular cases where noticeable effect of plastic spin on FLD is observed; $h_I^b/h_I = 0.999$; $L_{12} = 0$ outside the band.

strain direction x_1. This behavior is consistent with the experimental observations in Ref. Kim and Yin (1997). Consequently, the limit strain in this case is almost equal to the case for $\theta_I = 0^\circ$, as can be seen in Fig. 8(a). By contrast, in the case of no plastic spin ($q = 0$), no rotation of the orthotropic axes occurs outside the band, because the substructure spin ω_{12} is equal to $W_{12}(=0)$, although the orthotropic axes inside the band can rotate. However, in the cases of ①, the differences between θ and θ^b are quite small even at the localization point, both for $q = 0$ and for $q = -100$.

At the portions marked ②, ③, and ④ in Fig. 8, significant reductions of the limit strains are observed. The curves of θ and θ^b versus ε_{11} for these cases show a rather large misorientation between the orthotropic directions near the localization points, as can be observed in Fig. 9(a)–(c). The misorientation between θ and θ^b has a large effect on the occurrence of localization. In order to confirm this more clearly, several independent calculations have been carried out as discussed below.

All the calculations depicted in this paper have assumed the same initial orientations of orthotropy inside and outside the band, i.e. $\theta_I = \theta_I^b$. However, we have tried to assume different initial orientations

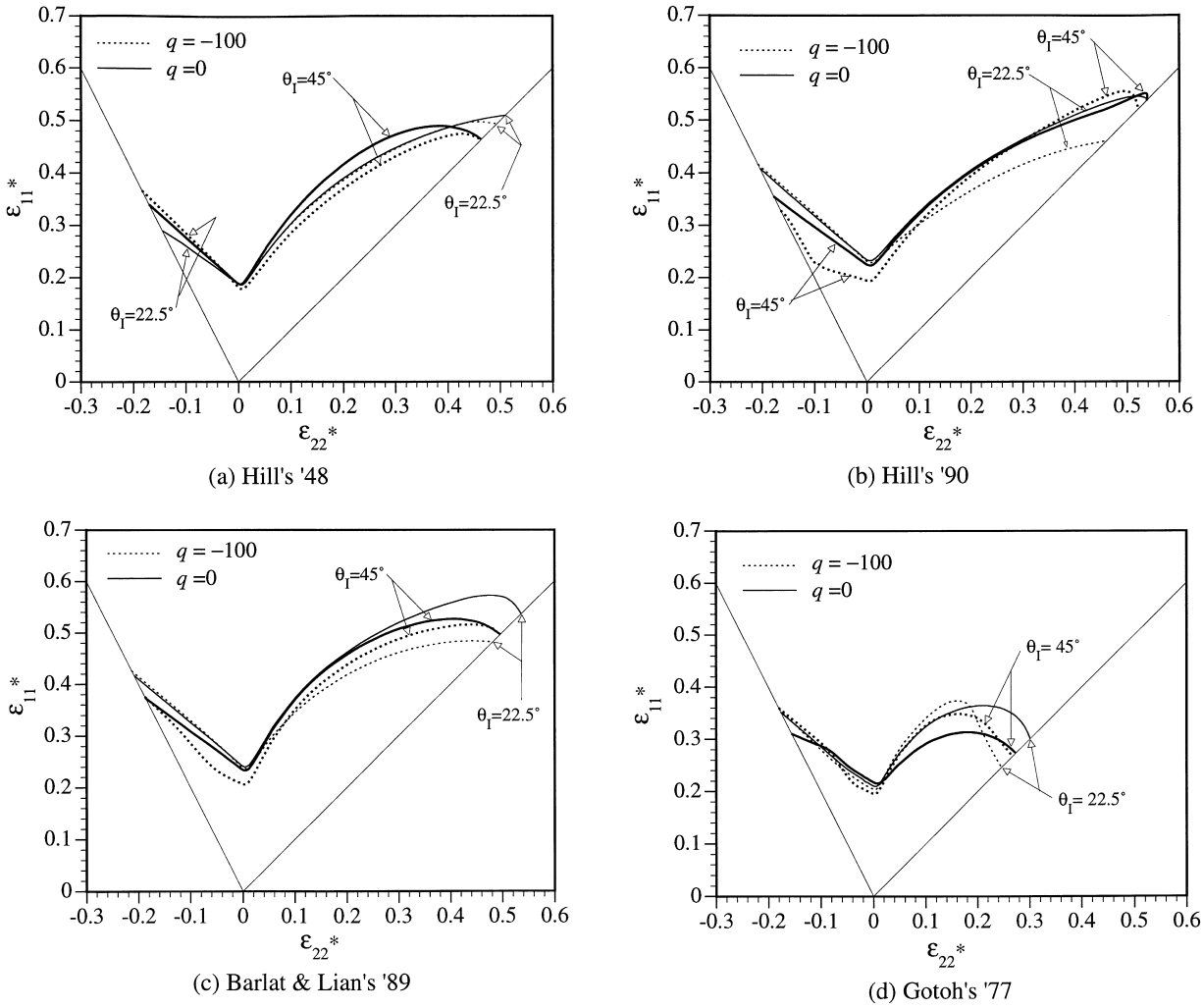

Fig. 10. Effect of plastic spin on FLD's; $h_I^b/h_I = 0.999$; $L_{12} \neq 0$ outside the band.

of orthotropy, i.e. $\theta_I \neq \theta_I^b$. As an example, for Hill's (1948) criterion, we assume $\theta_I = 10^\circ$ and $\theta_I^b = 6.6^\circ$ (these values almost correspond to the values found at the end of the computations for the case of $q = -100$ in Fig. 9(b), ③) with $\rho = 0$, $\psi_I = 0^\circ$ and $q = 0$. In this case, the localization strain, $\varepsilon_{11}^L = 0.172$, is obtained, and the final value of θ^b is 6.4°. On the other hand, if $\theta_I = \theta_I^b = 10^\circ$ is assumed, with all other conditions the same as before, $\varepsilon_{11}^L = 0.188$ is obtained. From these simple examples, we understand that misorientations of the orthotropic directions inside and outside the band can have a large effect on the occurrence of localization. In the presence of the plastic spin, the misorientation may evolve a great deal even from the standard condition $\theta_1 = \theta_I^b$, as was seen in Fig. 9, in particular Fig. 9(c).

In the case of Gotoh's (1977) criterion, the effect of plastic spin seems to be unrealistically large for $\rho > 0.4$. In this range of ρ, Gotoh's (1977) criterion predicts significantly smaller limit strains in comparison to the predictions of the other three criteria. This corresponds to the fact that the yield surface shape has been distorted more, as was seen in Fig. 2. The plastic spin employed here measures the noncoaxiality between the stress $\boldsymbol{\sigma}$ and the normal direction $\mathbf{N}^p$ to the yield surface. The more the yield surface shape is distorted, the more the $\boldsymbol{\sigma}$ and $\mathbf{N}^p$ tend to become noncoaxial. It seems that the value $q = -100$ is too large for the present case of Gotoh's (1977) criterion. Using the experimental data provided by Kim and Yin (1997), calibrations of the value of plastic spin coefficients for Gotoh's (1977) criterion could not be completed, because of a lack of data required for determining all the orthotropic coefficients A_1–A_9. According to the authors' knowledge, Kim and Yin's data is at present the only experimental evidence for the orientational evolution of anisotropy. It is also noted that, in Fig. 9(a), the curves for Hill's (1990) criterion with $q = -100$ (the case ②) first tend to rotate toward $\theta = 0^\circ$ and then toward $\theta = 90^\circ$. This behavior can be attributed to the evolution of anisotropy, i.e. in this yield criterion, the orthotropic coefficients are not constants, but evolve with increasing plastic deformation.

In Fig. 10(a)–(d), the effects of plastic spin are illustrated for the cases where shear straining ($L_{12} \neq 0$) is allowed for outside the band. In the range of negative values of ρ, the effects of plastic spin becomes slightly smaller. However, basically the effects seen in Fig. 10 are similar to those observed in Fig. 8.

5. Discussion

In M–K-model studies of necking in thin sheets, it is well known that the predictions show a strong influence of the yield criterion applied, and this is also found in the present investigation by comparison of four different anisotropic yield criteria. However, it is interesting to note here that the rather large differences are present even though all four yield criteria are fitted to approximately agree with the same set of experimental data. Another well known fact from previous M–K-model studies of sheet necking is that the predictions are strongly sensitive to the imperfection level, and this is illustrated in Fig. 3 for one of the four anisotropic yield criteria, but is otherwise not discussed here.

The non-symmetry of the forming limit diagrams with respect to the line $\rho = 1$ illustrated in Fig. 5 has usually not been found in M–K-model studies based on phenomenological plasticity models, even when anisotropic plasticity is accounted for. The same is true for the changes in band orientation near $\rho = 1$, where in fact several authors have assumed $\psi^* = 0^\circ$ a priori. However, with anisotropic plasticity, there is no material symmetry to guarantee that the change from $\psi^* = 0^\circ$ to $\psi^* = 90^\circ$ occurs exactly at $\rho = 1$, and in fact a more gradual change is found in Fig. 4(a). In the context of crystal plasticity this nonsymmetric behavior near $\rho = 1$ has been nicely illustrated and discussed by Wu et al. (1997, 1998).

The analyses for tension in directions inclined to the initial orthotropic axes of the anisotropy have shown that the predicted localization strains are quite sensitive to such deviations from the usual assumptions in M–K-model analyses. This sensitivity is different for the different anisotropic yield criteria (Fig. 5), and it cannot be expected that predictions for an intermediate angle as $\theta_I = 45^\circ$ are in between those for 0° and 90°. As would be expected, the deviations from the usual critical band

orientation, $\psi^* = 0^\circ$, near $\rho = 1$ are much more pronounced when the tensile directions are inclined to the initial orthotropic axes (Fig. 6(b)). For these types of loading it is also important to note the significant differences between the localization strains predicted when the conditions outside the band enforce zero shear strains, as compared to the situation where a shear strain is allowed for in order to enforce zero shear stress (Fig. 7). The results of these two sets of boundary conditions coincide when the tensile directions are along the orthotropic axes.

The effect of plastic spin has been incorporated in a few analyses here, as it has been shown in previous investigations that this improves the representation of experimentally observed changes in anisotropy orientation. Therefore, the effect of plastic spin is of most interest in the cases where the tensile directions are inclined to the initial orthotropic axes, so that the anisotropy rotates outside the band, as well as inside the band. It has been found (Figs. 8 and 10) that a realistic amount of plastic spin can result in localization strains that differ significantly from those predicted in the absence of plastic spin, and this is found for both types of boundary conditions, prescribing either zero shear strain or zero shear stress outside the band.

Acknowledgements

The authors wish to thank Professor Toshihiko Kuwabara of Tokyo University of Agriculture and Technology for helpful discussion from a viewpoint of experiments.

References

Asaro, R.J., Needleman, A., 1985. Texture development and strain hardening in rate dependent polycrystals. Acta Metall 33, 923–953.

Azrin, M., Backofen, W.A., 1970. The deformation and failure of a biaxially stretched sheet. Metall. Trans 1, 2857–2865.

Barlat, F., 1987. Crystallographic texture, anisotropic yield surfaces and forming limits of sheet metals. Mater. Sci. Eng 91, 55–72.

Barlat, F., Richmond, O., 1987. Crystallographic texture, anisotropic yield surfaces and forming limits of sheet metals. Mater. Sci. Eng 95, 15–29.

Barlat, F., Lian, J., 1989. Plastic behavior and stretchability of sheet metals. Part I: a yield function for orthotropic sheets under plane stress conditions. Int. J. Plasticity 5, 51–66.

Barlat, F., Lege, D.J., Brem, J.C., 1991. A six-component yield function for anisotropic materials. Int. J. Plasticity 7, 693–712.

Barlat, F., Maeda, Y., Chung, K., Yanagawa, M., Brem, J.C., Hayashida, Y., Lege, D.J., Matsui, K., Murtha, S.J., Hattori, S., Becker, R.C., Makosey, S., 1997. Yield function development for aluminum alloy sheets. J. Mech. Phys. Solids 45, 1727–1763.

Bassani, J.L., Hutchinson, J.W., Neale, K.W., 1979. On prediction of necking in anisotropic sheets. In: Lippmann, H. (Ed.), Metal Forming Plasticity: IUTAM Symposium Tutzing/Germany 1978. Springer–Verlag, Berlin, pp. 1–13.

Dafalias, Y.F., 1983. On the evolution of structure variables in anisotropic yield criteria at large plastic transformations. In: Boehler, J.P. (Ed.), Proceedings of the CNRS International Colloquium No. 351 — Failure Criteria of Structured Media – Villard de Lans, France, 1983. A.A. Balkema Publishers, Rotterdam, pp. 267–274 (finally published in 1993).

Dafalias, Y.F., 1985. The plastic spin. ASME J. Appl. Mech 52, 865–871.

Dafalias, Y.F., 1993. On multiple spins and texture development. Case study: kinematic and orthotropic hardening. Acta Mech 100, 171–194.

Dafalias, Y.F., 1998. Orientational evolution of plastic anisotropy. In: Khan, A.S. (Ed.), Proceedings of Plasticity '99: The Seventh International Symposium on Plasticity and Its Current Applications. Neat Press, Maryland, pp. 791–794.

Dafalias, Y.F., 1999. private communications.

Dafalias, Y.F., Rashid, M.M., 1989. The effect of plastic spin on anisotropic material behavior. Int. J. Plasticity 5, 227–246.

Gotoh, M., 1977. A theory of plastic anisotropy based on a yield function of fourth order (plane stress state)-I. Int. J. Mech. Sci 19, 502–512.

Hill, R., 1948. A theory of the yielding and plastic flow of anisotropic metals. Proc. Royal Soc. London 193A, 281.

Hill, R., 1950. Mathematical Theory of Plasticity. Clarendon Press, Oxford.

Hill, R., 1952. On discontinuous plastic states with special reference to localized necking in thin sheets. J. Mech. Phys. Solids 1, 19–30.
Hill, R., 1979. Theoretical plasticity of textured aggregates. Proc. Cambridge Philos. Soc 85, 179–191.
Hill, R., 1990. Constitutive modelling of orthotropic plasticity in sheet metals. J. Mech. Phys. Solids 38, 405–417.
Hill, R., 1993. A user friendly theory of orthotropic plasticity in sheet metals. Int. J. Mech. Sci 35, 19–25.
Hershey, A.V., 1954. The plasticity of an isotropic aggregate of anisotropic face centered cubic crystals. ASME J. Appl. Mech 21, 241–249.
Hoferlin, E., Van Bael, A., Hiwatashi, S., Van Houtte, P., 1998. Influence of texture and microstructure on the prediction of forming limit diagram. In: Carstensen, J.V. (Ed.), Proceedings of the 19th Risø International Symposium on Materials Science. Risø National Laboratory, Roskilde, Denmark, pp. 291–297.
Hosford, W.F., 1972. A generalized isotropic yield criterion. ASME J. Appl. Mech 39, 607–609.
Keeler, S.P., 1968. Understanding sheet metal formability, Parts I–VI, Machinery 74.
Kim, K.H., Yin, J.J., 1997. Evolution of anisotropy under plane stress. J. Mech. Phys. Solids 45, 841–851.
Kuroda, M., 1997. Interpretation of the behavior of metals under large plastic shear deformations: a macroscopic approach. Int. J. Plasticity 13, 359–383.
Kuwabara, T., Ikeda, S., Kuroda, K., 1998a. Measurement and analysis of differential work hardening in cold-rolled steel sheet under biaxial tension. J. Mater. Proc. Tech 80/81, 517–523.
Kuwabara, T., Susuki, I., Ikeda, S., 1998b. Identification of a yield locus of aluminum alloy sheet A5182-O by biaxial tensile tests using cruciform specimens. Journal of JSTP 89, 56–61 (in Japanese with English abstract).
Lee, H., Im, S., Atruli, S.N., 1995. Strain localization in an orthotropic material with plastic spin. Int. J. Plasticity 11, 423–450.
Lian, J., Barlat, F., Baudelet, B., 1989a. Plastic behavior and stretchability of sheet metals. Part II: effect of yield surface shape on sheet forming limit. Int. J. Plasticity 5, 131–147.
Lian, J., Zhou, D., Baudelet, B., 1989b. Application of Hill's new yield theory to sheet metal forming. Part I: Hill's 1979 criterion and its application to predicting sheet forming limit. Int. J. Mech. Sci 31, 237–247.
Logan, R.W., Hosford, W.F., 1980. Upper-bound anisotropic yield locus calculations assuming ⟨111⟩-pencil glide. Int. J. Mech. Sci 22, 419–430.
Marciniak, Z., Kuczynski, K., 1967. Limit strains in the process of stretch forming sheet metal. Int. J. Mech. Sci 9, 609–620.
Needleman, A., Tvergaard, V., 1984. Limits to formability in rate-sensitive metal sheets. In: Carlsson, H., Ohlson, N.G. (Eds.), Mechanical Behaviour of Materials-IV. Pergamon Press, Oxford, New York, pp. 51–65.
Parmar, A., Mellor, P.B., 1978. Predictions of limit strains in sheet metal using a more general yield criterion. Int. J. Mech. Sci 20, 385–391.
Støren, S., Rice, J.R., 1975. Localized necking in thin sheets. J. Mech. Phys. Solids 23, 421–441.
Tvergaard, V., 1978. Effect of kinematic hardening on localized necking in biaxially stretched sheets. Int. J. Mech. Sci 20, 651–658.
Tvergaard, V., 1980. Bifurcation and imperfection-sensitivity at necking instabilities. ZAMM 60, T26–T34.
Tvergaard, V., 1989. Plasticity and creep at finite strains. In: Germain, P., Piau, M., Gaillerie, D. (Eds.), Theoretical and Applied Mechanics. Elsevier, Amsterdam, pp. 349–368 (IUTAM, 1989).
Tvergaard, V., Needleman, A., 1993. Shear band development in polycrystals. Proc. Royal Soc. London 443A, 547–562.
Wu, P.D., Neale, K.W., Van der Giessen, E., 1997. On crystal plasticity FLD analysis. Proc. Royal Soc. London 453A, 1831–1848.
Wu, P.D., Neale, K.W., Van der Giessen, E., Jain, M., Makinde, A., MacEwen, S.R., 1998. Crystal plasticity forming limit diagram analysis of rolled aluminum sheets. Metall. Mater. Trans 29A, 527–535.
Xu, S., Weinmann, K.J., 1998. Prediction of forming limit curves of sheet metals using Hill's 1993 user friendly yield criterion of anisotropic materials. Int. J. Mech. Sci 40, 913–925.